

**Evolving roles and dynamics for catch and slip bonds during adhesion cluster maturation**Elizaveta A. Novikova <sup>1,2</sup> and Cornelis Storm <sup>2,3</sup><sup>1</sup>*Institute for Integrative Biology of the Cell (I2BC), CEA, CNRS, Université Paris-Sud, Université Paris-Saclay, 91198 Gif-sur-Yvette Cedex, France*<sup>2</sup>*Department of Applied Physics, Eindhoven University of Technology, P.O. Box 513, NL-5600 MB Eindhoven, The Netherlands*<sup>3</sup>*Institute for Complex Molecular Systems, Eindhoven University of Technology, P.O. Box 513, NL-5600 MB Eindhoven, The Netherlands*

(Received 23 August 2019; revised 23 December 2020; accepted 12 February 2021; published 3 March 2021)

Focal adhesions are the loci of cellular adhesion to the extracellular matrix. At these sites, various integrins forge connections between the intracellular cytoskeleton and the outside world; large patches of multiple types of integrins together grip hold of collagen, fibronectin, and other extracellular matrix components. A single focal adhesion will likely contain bonds whose lifetime increases with applied load (catch bonds), and bonds whose lifetime decreases with applied load (slip bonds). Prior work suggests that the combination of different types of integrins is essential for focal adhesion stability and mechanosensory functionality. In the present work, we investigate numerically the interplay between two distinct types of bonds, and we ask how the presence of slip bonds, in the same focal integrin cluster, augments the collective behavior of the catch bonds. We show that mixing these two components may increase the low-force mechanical integrity that may be lacking in pure-catch adhesions, while preserving the potential to strengthen the entire adhesion when a force is applied. We investigate the spatial distribution in mixed-integrin focal adhesions, and we show that the differential response to loading leads, via an excluded volume interaction, to a dependence of the individual integrin diffusivities on the applied load, an effect that has been reported in experiments.

DOI: [10.1103/PhysRevE.103.032402](https://doi.org/10.1103/PhysRevE.103.032402)**I. INTRODUCTION**

Cells are able to sense and react to the stiffness of the extracellular environment [1–3]. Through their focal adhesions (FAs), cells are able to confer mechanical forces onto the extracellular matrix (ECM) to move around, or to probe their surroundings. Inside each FA transmembrane, proteins called integrins provide direct links between the cells' internal contractile machinery and various ECM components [4,5]. Integrins are heterodimers, composed of two subunits called  $\alpha$  and  $\beta$ ; each of these comes in various kinds. Together, there are about 25 different integrins in the vertebrates, allowing their cells to form robust adhesions to ECM components such as collagen, fibrin(ogen), fibronectin, and vitronectin.

Given that there are so many different types of integrins, it is no surprise that multiple types may be present within the same focal adhesion [6]. For this paper, we will focus on the pair of integrins  $\alpha_5\beta_1$  and  $\alpha_V\beta_3$ , both of which bind to the extracellular ligand fibronectin [4]. These two species colocalize within the same focal adhesion [7,8], their signaling pathways interfere [9], and their roles in adhesion and motility complement each other [7,8,10]. More generally, interactions—direct or indirect—between integrins of different types have been implicated in guiding force generation and rigidity sensing [11], but the  $\alpha_5\beta_1$  and  $\alpha_V\beta_3$  pair in particular has been repeatedly conjectured to act cooperatively in adhesion maturation and cell spreading. Interestingly,  $\alpha_5\beta_1$  and  $\alpha_V\beta_3$  show very different responses to mechanical loading.

The bond between  $\alpha_5\beta_1$  and fibronectin was among the first integrin-ligand pairs for which catch bonding—a counterintuitive behavior in which the lifetime of the bond initially rises with the applied force—was demonstrated [12]. Although the same paper suggests that (ionic) conditions may interfere with the catch-bonding behavior, there is little doubt that  $\alpha_5\beta_1$  may be reliably characterized as a single-molecular catch bond former. The story is less clear for the bond between  $\alpha_V\beta_3$  and fibronectin. At a *collective* level,  $\alpha_V\beta_3$  has been shown to form a slip bond—a “regular” connection for which the lifetime monotonically decreases with the applied force—with fibronectin [13], but these results do not necessarily support a similar claim at the single-bond level. Jiang *et al.* likewise demonstrate a clear  $\alpha_V\beta_3$ -mediated single-molecule slip bond between fibronectin and the cytoskeleton [14], but they also show that talin (which in physiological settings may be expected to be present) is crucial for this behavior. Both of these findings appear at odds with what is reported in [15], which shows strong evidence of a single-molecular  $\alpha_V\beta_3$  catch bond. Another  $\beta_3$  integrin,  $\alpha_{IIb}\beta_3$ , which binds fibrinogen in platelets, was shown to be a very robust single-molecule slip bond former [16]. Summarizing these findings, we conclude that while there is currently no unambiguous experimental confirmation that catch and slip bonds are present in the same FA, the broad range of behaviors of both  $\alpha_5\beta_1$  and  $\alpha_V\beta_3$  supports the assumption that there are operational regimes in which this is likely the case. Given the fact that  $\alpha_5\beta_1$  and  $\alpha_V\beta_3$  are both needed for healthy adhesion, this motivates us to study here, in a computational model, the

effects that these two types of bonds have on each other when they are present within the same FA domain.

This approach is not new. To better understand the roles of integrins in adhesion, models of the mechanosensing and mechanotransduction mechanisms on the level of the cell [17,18] and on the level of focal adhesion [11,19–21] were previously developed. In this work, we consider a focal adhesion with two types of integrins, complementing the experimental findings in [11] with a theoretical analysis of mixed cluster stability and a model for integrin mobility inside the focal adhesion. Our results exploit and extend our previous simulations [22], in which we considered mechanosensing by catch bond clusters. The central question that we ask here is very different: How does the force, exerted on focal adhesion, affect the binding lifetimes of individual integrins in mixed load-sharing clusters, and what light can the diffusivity of integrins inside the focal adhesion shed on this behavior? To answer it, we consider the force-response of a focal adhesion consisting of two integrin types exposed to a constant external load. Using the assumption of uniform load sharing, we determine equilibrium binding probabilities for each species individually in such a mixed cluster, as a function of the individual properties of the bonds inside it, and of the composition of the cluster. We explore the stability of a mixed cluster under load and then include simple lateral diffusion of integrins on a two-dimensional lattice. We determine the diffusivity of free (unbound) integrins as a function of the applied force, and we demonstrate that the diffusivity of integrins inside a focal adhesion can be used as a macroscopic reporter for the force exerted on it.

## II. BINDING AND UNBINDING OF SINGLE CATCH AND SLIP BONDS

The binding and unbinding rates  $k_b$  and  $k_u$  characterize the equilibrium kinetics of a single, noncovalent molecular bond. These rates are load-dependent; in response to an applied pulling force  $f$ , the unbinding rate of so-called *slip bonds* is predicted, according to Kramer's rate theory [23], to increase exponentially as

$$k_u^{\text{sb}} = k_0^{\text{sb}} \exp\left(\frac{+f\xi_{\text{sb}}}{k_B T}\right). \quad (1)$$

In this expression,  $\xi_{\text{sb}}$  is a microscopic unbinding length,  $k_B$  is the Boltzmann constant, and  $T$  is the absolute temperature.  $k_0^{\text{sb}}$  is the unforced unbinding rate, i.e., the rate at which the bond opens up under the effect of spontaneous fluctuations. It is set by an attempt frequency  $k_0$  and by  $\Delta U_{\text{sb}}$ , the height of the energetic barrier corresponding to the dissociation of the bond,

$$k_0^{\text{sb}} = k_0 \exp\left(\frac{\Delta U_{\text{sb}}}{k_B T}\right). \quad (2)$$

In the case of a catch bond, the unbinding behavior [24] is quite different: When a moderate tension is applied to this bond, the bond dissociation rate initially *decreases*, corresponding to an increase in the single-bond lifetime. Using the so-called ‘‘two pathway model’’ [25], a simplified way to capture a nonmonotonous dependence of the lifetime on the applied force, the total unbinding rate of such a catch bond

may be computed as

$$k_u^{\text{cb}} = k_{0,1}^{\text{cb}} \exp\left(\frac{+f\xi_1}{k_B T}\right) + k_{0,2}^{\text{cb}} \exp\left(\frac{-f\xi_2}{k_B T}\right), \quad (3)$$

that is, as a sum of two rates corresponding to two parallel dissociation processes. Process 1 (with unforced unbinding rate  $k_{0,1}$  and dissociation length  $\xi_1$ ) describes dissociation along a sliplike path, as may be surmised from the increase in rate with increasing force. Process 2 (with unforced unbinding rate  $k_{0,2}$  and dissociation length  $\xi_2$ ) describes dissociation along a catch path, different in the sense that the force dependence in the exponent carries a minus sign, which leads to a decreasing catch unbinding rate with increasing force.

Following the procedure detailed in [22], we reexpress Eq. (3) in terms of a normalized catch bond unbinding rate  $k_u^{\text{cb}}(\phi)$ , under the assumption that the dissociation lengths for the two pathways are the same. This assumption is motivated in part by the fact that these two dissociation lengths correspond to unbinding pathways of the same molecular complex, and are therefore determined by the size and flexibility of the same integrin-ligand complex, which suggests that  $\xi_1$  and  $\xi_2$  must be similar in magnitude. For this reason, but also to limit the amount of free parameters, we therefore set  $\xi_1 = \xi_2 \equiv \xi_{\text{cb}}$ , with  $\xi_{\text{cb}}$  the average of  $\xi_1$  and  $\xi_2$ . All forces are then nondimensionalized using  $\phi = f\xi_{\text{cb}}/k_B T$ , and the unforced rates are rewritten as

$$k_{0,1}^{\text{cb}} \equiv \kappa_0 e^{-\phi_1}, \quad k_{0,2}^{\text{cb}} \equiv \kappa_0 e^{\phi_1}. \quad (4)$$

We may set the reference rate to  $\kappa_0 = 1 \text{ s}^{-1}$  without loss of generality, and from now on we will nondimensionalize all rates using this number:  $k \rightarrow k/\kappa_0$ . Going through these steps results in a two-parameter representation of the catch bond, in which  $\phi_1$  and  $\phi_2$  reflect, respectively, the dissociation energy barriers for the slip and the catch path:

$$k_u^{\text{cb}}(\phi) = e^{(\phi-\phi_1)} + e^{-(\phi-\phi_2)}. \quad (5)$$

In the present work, we aim to combine these catch bonds with slip bonds. Their unbinding rate is given by Eq. (1) which, in the exact same manner, may be reexpressed in terms of nondimensional forces and rates

$$k_u^{\text{sb}}(\phi) = e^{(\phi/\rho_\xi - u_{\text{sb}})}, \quad (6)$$

with two additional parameters:  $\rho_\xi = \xi_{\text{cb}}/\xi_{\text{sb}}$  is the ratio of the catch and slip bond dissociation lengths, and  $u_{\text{sb}} = -\Delta U_{\text{sb}}/k_B T$  sets the unforced unbinding rate of the slip bond. Since we will be varying it throughout this paper, a brief note on the interpretation of  $\rho_\xi$  is in order: While technically it is the ratio of the two dissociation lengths, it may equivalently be considered a measure for the relative strength of the slip bonds in the system. Low values  $\rho_\xi \approx 1$  mean slip bonds break at far lower forces than the catch bonds do, while higher values  $\rho_\xi \gtrsim 5$  mean slip bonds break concurrently or even only at higher forces than the catch bonds. For this reason, we will be referring to  $\rho_\xi$  as the *relative slip bond strength*. Once its unbinding rate  $k_u(\phi)$  is known, the average lifetime  $\tau(\phi)$  of a single bond is then computed as

$$\tau(\phi) \equiv \frac{1}{\kappa_0 k_u(\phi)}. \quad (7)$$

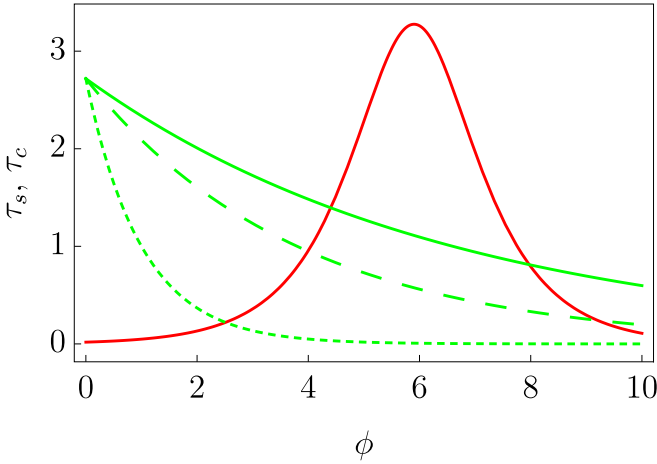


FIG. 1. Average lifetimes  $\tau_c, \tau_s$  of catch and slip bonds as a function of the dimensionless force  $\phi$ . Throughout this paper, green points and curves will correspond to slip-bond data, and red points and curves will correspond to catch-bond data. Parameter values for the catch bonds [described by Eq. (5)] are as follows:  $f^* = 5.38$  pN,  $\phi_1 = 7.78$ , and  $\phi_2 = 4.02$ . Parameter values for the slip bonds [described by Eq. (6)] are as follows: short dashed,  $\rho_\xi = 1$ ; long dashed,  $\rho_\xi = 3.8$ ; solid line,  $\rho_\xi = 6.6$ . In all cases, we set  $u_{sb} = 1$ .

Since their discovery, single biological catch bonds have received considerable attention in the community. Recent experiments [12,26,27] measured catch-bond characteristics by pulling a single receptor-ligand bond with an AFM tip. In this work, we use the parameters of an individual integrin-fibronectin catch bond, which were obtained in one of these experiments [12]. As earlier in [22], we use the two-pathway model from [25], and we fit it to the data from [12], using  $f^*, \phi_1$  and  $\phi_2$  as our two fit parameters. We note that the experimental data are richer than what can be captured by a simple two-pathway model. Double-exponential models will likely do a better job, but for now we are interested mainly in exploring the advantages offered by general catch bonding, as evidenced by nonmonotonic force-lifetime relations. In the interest, again, of limiting the number of free parameters, we will therefore stick to the two-pathway approach. Best-fit parameters for the catch bond were determined to be  $f^* = 5.38$  pN,  $\phi_1 = 7.78$ , and  $\phi_2 = 4.02$ . As also noted in [11], and detailed in the Introduction, compared to catch bonds the potential slip bonds formed by the integrins we consider here have not been studied in as much detail. When they have been quantified, the parameters that characterize their monotonically decreasing force-lifetime curves show a broad range of typical timescales. For demonstrational purposes, in the present paper we will fix the catch-bond parameters at the aforementioned values, and we will vary the slip-bond parameter  $\rho_\xi$  to determine the importance of the relative slip-bond strength. Throughout this paper, we set  $u_{sb} = 1$  as the reference zero-force unbinding rate for slip bonds. In Fig. 1, we plot the resulting catch and slip lifetimes for various values of  $\rho_\xi$ . The distinct force-lifetime responses are clearly visible with the catch bond showing the characteristic maximum at finite force at the unbinding lifetime and the slip bonds showing longer lifetimes for higher values of  $\rho_\xi$ . With these

preliminaries in place, we turn to the behavior of a mixed cluster containing both catch and slip bonds, at finite force.

### III. A MIXED CATCH-SLIP CLUSTER AT FIXED FORCE: MEAN FIELD THEORY

Following the approach laid out in Schwarz *et al.* [19], we consider a fixed total number of integrin receptors (bound or unbound)  $N_t$ , out of which  $N_{ct}$  are catch bonds and  $N_{st}$  are slip bonds;  $N_{ct}$  and  $N_{st}$  are individually conserved. We will let  $i$  denote the number of bound catch receptors, and  $j$  denotes the number of bound slip receptors at time  $t$ . We denote the probability of having  $i$  closed catch receptors and  $j$  closed slip receptors at a given time  $t$  by  $p_{i,j}(t)$ ; its evolution is governed by a one-step, two-variate master equation:

$$\begin{aligned} \frac{dp_{i,j}(t)}{dt} = & r_{i,j+1}^s(F_t)p_{i,j+1} + r_{i+1,j}^c(F_t)p_{i+1,j} \\ & + g_{i-1,j}^c p_{i-1,j} + g_{i,j-1}^s p_{i,j-1} \\ & - [r_{i,j}^c(F_t) + r_{i,j}^s(F_t) + g_{i,j}^c + g_{i,j}^s] p_{i,j}, \quad (8) \end{aligned}$$

where  $r^{s/c}(F)$  are the force-dependent unbinding rates for slip ( $s$ ) and catch ( $c$ ) bonds, and  $g^{s/c}$  are the rebinding rates setting the typical time for the formation of a new catch or slip attachment to an extracellular ligand.  $F_t$  is the total force applied to all bonds. As such, the first line of the right-hand side (RHS) of Eqs. (8) describes the change in  $p_{i,j}(t)$  due to the unbinding of either a catch or a slip bond from a state with one additional bound receptor compared to  $\{i, j\}$ , the second line represents rebinding of either a catch or a slip bond from a state with one fewer bound receptor compared to  $\{i, j\}$ , and the third line represents unbinding *and* rebinding of either type of receptor from the state  $\{i, j\}$  itself. Equation (8) describes a stochastic process underlying the temporal evolution of the probability distribution  $p_{i,j}(t)$ . Derived from it are the quantities in which we will initially be most interested, namely the expectation values for the total number of bound receptors  $N$ , and those for the numbers of bound catch ( $N_c$ ) and slip receptors ( $N_s$ ) individually,

$$\begin{aligned} N_c(t) &\equiv \langle i \rangle(t) = \sum_{\{i,j\}} i p_{i,j}(t), \\ N_s(t) &\equiv \langle j \rangle(t) = \sum_{\{i,j\}} j p_{i,j}(t), \\ N(t) &\equiv \langle i + j \rangle(t) = \sum_{\{i,j\}} (i + j) p_{i,j}(t). \quad (9) \end{aligned}$$

We now assume that the rebinding rates  $g$  are force-independent since they involve the (re)formation of a bond between a receptor and a ligand, which are not connected and therefore do not take part in transmitting the mechanical load. This suggests that they can generally associate in a stress-free conformation; only after it closes can the bond begin to “sense” the load. Given that the load-sharing geometry in FAs is mostly planar, with all bonds acting in parallel, we believe this to be a reasonable assumption. This helps simplify the initial conditioning of the system, and although it may be necessary to revisit this assumption to permit quantitative analysis, we are, for the purpose of this paper, interested first

in establishing the qualitative effects of mixing slip and catch bonds in adhesive clusters. Force-independent rebinding is enforced by setting

$$\begin{aligned} g_{i,j}^c &= g_i^c = k_0 \gamma (N_{ct} - i), \\ g_{i,j}^s &= g_j^s = k_0 \gamma (N_{st} - j), \end{aligned} \quad (10)$$

i.e., rebinding is proportional to the instantaneous number of available, unbound receptors of the same type. Again, we simplify the system by assuming that  $\gamma$  is independent of the force, and is the same for both types of bond. Of course, there is no reason for this to hold in real life; the kinetics of integrin-ligand bond formation will differ by type.

The force-dependent unbinding rates  $r^s(F)$  and  $r^c(F)$  are where the differential characteristics of catch and slip bonds manifest themselves. From now on we describe the process in terms of the total dimensionless force  $\Phi = F_i/f^*$ , and we define

$$\begin{aligned} r_{i,j}^c(\Phi) &= r_i^c(\Phi) \equiv i k_0 k_u^{cb}(\bar{\phi}), \\ r_{i,j}^s(\Phi) &= r_j^s(\Phi) \equiv j k_0 k_u^{sb}(\bar{\phi}), \end{aligned} \quad (11)$$

where the normalized rates  $k_u^{cb}$  and  $k_u^{sb}$  are evaluated at the average loading force, which we obtain by assuming a uniform distribution of the total load across all bound receptors, i.e.,

$$\bar{\phi} = \frac{\Phi}{i+j}. \quad (12)$$

Nonuniformly distributed load may well be present in focal adhesions, and may be implemented by a spatially varying distribution of  $\Phi$ ; again, we start from the simplest scenario here. With these conventions, we derive directly from Eq. (8) an evolution equation for  $N(t)$ , the equilibrium number of bound receptors

$$\frac{d}{dt}N = \sum_{(i,j)} (i+j) \left( \frac{dp_{i,j}}{dt} \right) = -\langle r_{i,j}^c \rangle + \langle g_{i,j}^c \rangle - \langle r_{i,j}^s \rangle + \langle g_{i,j}^s \rangle, \quad (13)$$

where the summation is over all of the possible numbers  $\{i, j\}$  of bound catch and slip bonds in a cluster, and  $\langle \rangle$  denotes averages in the distribution  $p_{i,j}(t)$ . Equation (13) can be split into two separate equations, describing the equilibrium number of catch  $N_c = \langle i \rangle$  and slip  $N_s = \langle j \rangle$  bonds separately. Assuming that all rate functions vary slowly around their equilibrium values, we make the mean field approximation by replacing  $\langle r_{i,j}^c \rangle$ ,  $\langle r_{i,j}^s \rangle$ ,  $\langle g_{i,j}^c \rangle$ , and  $\langle g_{i,j}^s \rangle$  by the first terms in their Taylor expansions around  $\{\langle i \rangle, \langle j \rangle\}$ :  $\langle r_{i,j}^c \rangle \approx r_{(\langle i \rangle, \langle j \rangle)}^c$ ,  $\langle g_{i,j}^c \rangle \approx g_{(\langle i \rangle, \langle j \rangle)}^c$ , etc. This transforms Eqs. (13) into the following coupled system:

$$\begin{aligned} \frac{d}{dt}N_c &= -N_c k_u^{cb} \left( \frac{\Phi}{N_c + N_s} \right) + \gamma (N_{ct} - N_c), \\ \frac{d}{dt}N_s &= -N_s k_u^{sb} \left( \frac{\Phi}{N_c + N_s} \right) + \gamma (N_{st} - N_s). \end{aligned} \quad (14)$$

Here the time  $t$  is actually the nondimensionalized time  $t\kappa_0$ , but as mentioned we have set  $\kappa_0 = 1 \text{ s}^{-1}$ . Note, also, the nature of the coupling: In our model, the different types of bonds are aware of each other only through the shared total force  $\Phi$ . At equilibrium, the RHSs of both equations in the

system above vanish. At zero overall force, the equations fully decouple. For general forces, the coupled system of Eqs. (14) has two solutions for each value of force. One of the solutions is unstable, while the other corresponds to the local equilibrium and is stable. These two solution branches are readily obtained by direct numerical solution of Eqs. (14), with their RHSs equated to zero.

As shown in the panels in the left-hand column of Fig. 2, the critical force for cluster unbinding becomes greater as  $\rho_\xi$  is increased. All else being equal, we are simply adding more resilient slip bonds which increase the strength of the entire cluster. Also visible is that in equilibrium, the effect of mixing catch and slip bonds is that slip bonds provide most of the adhesion at low forces, while the catch bonds take over at intermediate and high forces. This is a marked change in functionality over having just catch bonds; while these are able to stabilize adhesions at high forces, they must pass through an extended, weakly bound regime to get there. Mixed catch-slip adhesion clusters always have an appreciable number of the integrins bound, and as such they provide stability at all force levels. We note, however, that while this *changes* the functionality of the mixed cluster compared to a purely catch or slip system, the enhanced stability is not necessarily an improvement in functionality. Particularly in mechanosensory processes, cells may actually benefit from the ability to rapidly form, break, and reform transient connections to the substrate. We now compare these numerical solutions to the results of stochastic simulations of the mixed bonds system.

#### IV. STOCHASTIC SIMULATIONS OF MIXED CLUSTERS: EQUILIBRIUM BOND NUMBERS

While the mean field approximation can teach us something about equilibrium behavior and expectation values, it says nothing about the dynamic behavior, and in particular it is not able to address the lifetime of the stable state. As we have demonstrated in earlier work [22], the mechanism for cluster unbinding is fluctuation-driven, and what we have called the stable solution branch is actually a metastable branch. A sufficiently large bond number fluctuation—which will come along at some point—prompts unbinding of the entire cluster. To address the lifetime of mixed clusters, we therefore turn to stochastic simulations, for which we use the Gillespie algorithm [22,28]. We initiate the system at a certain total number of bound receptors of each type, and we specify the cluster composition (total numbers of available catch and slip bonds). The choice of the initial value of bound receptors determines the typical evolution of the simulation, in the sense that in order to reach the (meta)stable solution branch, the initial values must be chosen within the basin of attraction of that branch. A typical simulation allows us to compute the typical evolution of the number of bound catch and slip bonds with time, as Fig. 2 demonstrates. The solid lines are the equilibrium predictions from Eqs. (14), and indeed the system is seen to converge onto the predicted values after a brief equilibration period. For these particular choices of parameters, the cluster is stable over the entire time of the simulation. However, the stochastic simulations also capture cluster unbinding; if we simulate for a sufficiently long

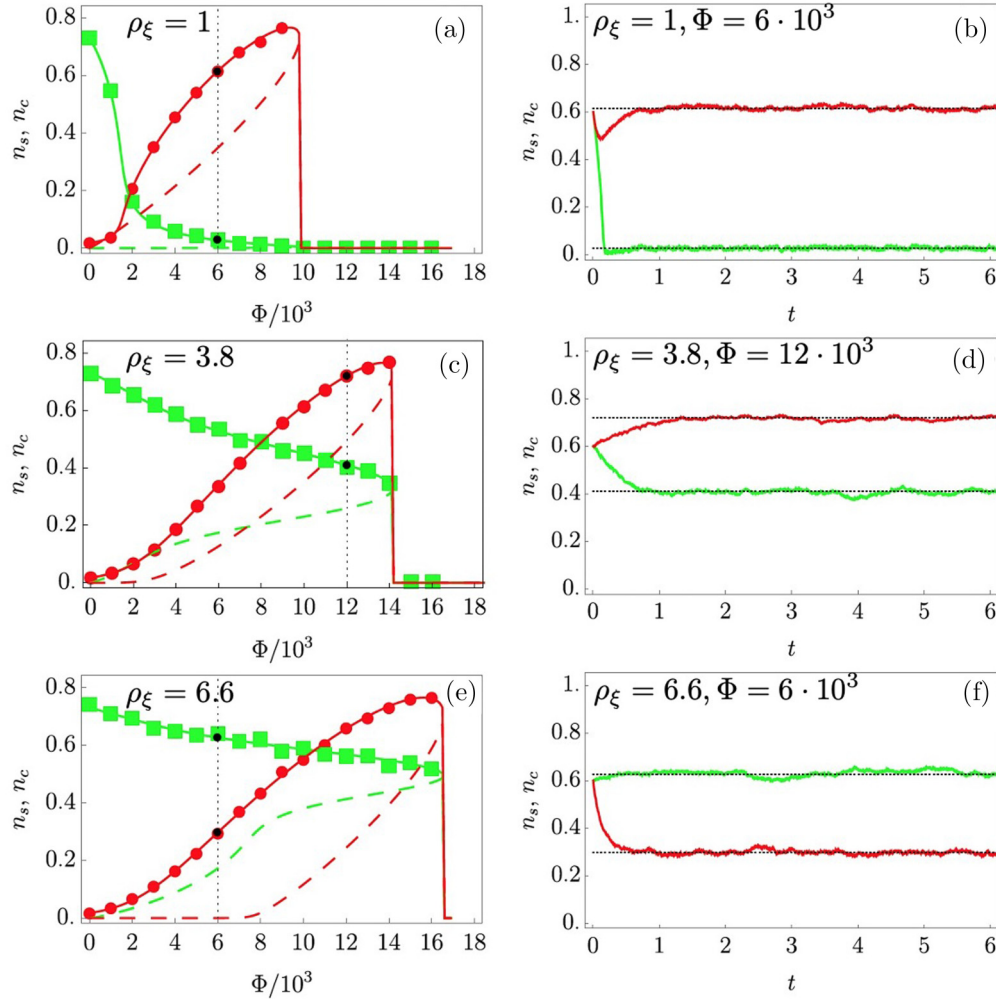


FIG. 2. (a), (c), and (e) Relative fractions of closed catch ( $n_c$ , red) and slip ( $n_s$ , green) bonds as a function of the total scaled force  $\Phi$  for relative slip bond strengths  $\rho_\xi = 1$  (a),  $\rho_\xi = 3.8$  (c), and  $\rho_\xi = 6.6$  (e), respectively. Points represent simulation results, while solid lines graph the deterministic solution obtained by solving Eqs. (14). (b), (d), and (f) Evolution of the relative fractions of closed catch ( $n_c$ ) and slip ( $n_s$ ) bonds as a function of time at a fixed force for relative slip bond strengths  $\rho_\xi = 1$  (b),  $\rho_\xi = 3.8$  (d), and  $\rho_\xi = 6.6$  (f), respectively. Bound fractions for both catch and slip bonds were initialized at 0.6. The fixed force chosen to run the temporal simulation is represented by the vertical lines in the curves on the right (at  $\Phi = 6 \times 10^3$ ,  $\Phi = 12 \times 10^3$ , and  $\Phi = 6 \times 10^3$  for the three respective values of  $\rho_\xi$ ); in each graph on the left, the two black dots where the vertical line intersects the stable branches for catch and slip bonds represent the predicted equilibrium binding fractions; these are indicated with horizontal dotted lines in the graphs on the right verifying that indeed the system tends to its predicted stable equilibrium. All of the simulations were done for a system of 2048 catch bonds and 2048 slip bonds, with a rebinding rate  $\gamma = 1$ , and at  $u_{sb} = 1$ .

time, an initially stabilized cluster will unbind after a spontaneous supercritical bond number fluctuation. Repeating these simulations multiple times, for different total forces and different parameter values, we collect statistics on both the average values of the number of bound receptors of each type, and the lifetime of the composite cluster. Figure 2 shows that, as predicted by the mean-field model, the average relative numbers of bound catch [ $n_s = \langle N_s(t) \rangle_t / N_{st}$ ] and slip [ $n_c = \langle N_c(t) \rangle_t / N_{ct}$ ] bonds in a stable adhesive cluster follows the expected behavior, and that catch and slip bonds preserve their tendencies even when coupled to each other via the force applied to a composite cluster. The number of catch bonds still peaks at some finite forces, while the equilibrium fraction of bound slip bonds decreases monotonically with increasing force. In measuring these average bound receptor

numbers, we take into account only the times during which a stable adhesion is present; should the cluster unbind, we stop measuring. Thus, what this simulation is bearing out is that the composition of stably adherent clusters is reliably predicted by Eqs. (14).

## V. STOCHASTIC SIMULATIONS OF MIXED CLUSTERS: CLUSTER LIFETIMES

With the force-dependent numbers of bound receptors and their partitioning between catch and slip now clear, we may ask what additional functionality, if any, the presence of both types of bonds offers over only a single species of integrin. Is it true that the increased presence of bound receptors (mostly slip) at low forces translates into increased lifetimes in this

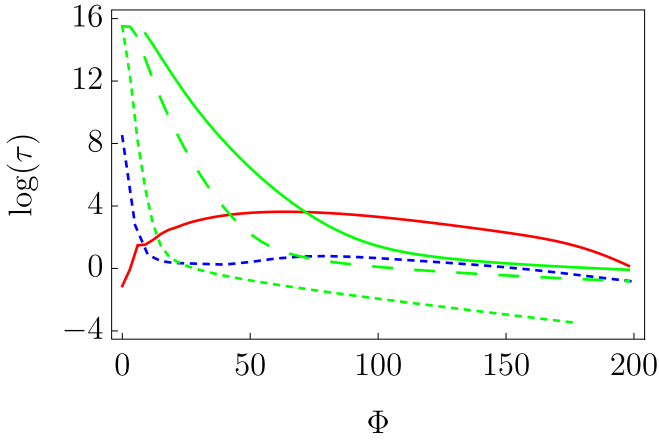


FIG. 3. Comparison between the analytically predicted lifetimes  $\tau$  as a function of the total force  $\Phi$  of a pure-catch cluster (red curve, for a cluster with 100 catch bonds and 0 slip bonds), three pure-slip clusters at different relative slip bond strengths (green curves: short-dashed,  $\rho_\xi = 1$ ; long-dashed,  $\rho_\xi = 3.8$ ; solid line,  $\rho_\xi = 6.6$ ; in each case for a cluster consisting of 100 slip bonds and 0 catch bonds), and a mixed cluster with 50 slip bonds and 50 catch bonds (blue curve,  $\rho_\xi = 1$ ). All curves have  $\gamma = 0.2$  and  $u_{sb} = 1$ .

region, and is this providing additional and previously missing low-force stability? Our analytical computations (detailed in the Appendix [Eq. (A1)]) allow us to calculate the lifetime of a mixed cluster, and compare it to the lifetimes of clusters containing only catch or only slip bonds. Representative illustrations of these analytical results are collected in Fig. 3.

As Fig. 3 illustrates, mixing catch and slip bonds provides additional functionality compared to either of the two single-component systems. At low forces, the slip bonds provide initial stability to a nascent cluster compared to a catch-only cluster. This eliminates the weakly bound low-force regime from the pure catch system; the slip bonds ensure immediate and effective adhesion. As the force rises, and slip bonds are gradually replaced by catch bond integrins, the behavior of the entire cluster increasingly reflects their high-force stabilizing effect; the blue curve is above the green curve. The different behavior in mixed clusters is thus obvious from the mean lifetime; the catch bonds in the mixed cluster provide additional stability and a far higher threshold force for unbinding at high forces compared to pure slip bond systems, while the slip bonds provide greatly enhanced stability at lower forces.

That the lifetime of the mixed cluster is nowhere longer than either the pure catch or the pure slip system should not come as a surprise; in the regimes where the behavior of one type of bond dominates, this behavior is always going to be diluted to some extent by the presence of the other, subdominant bond type.

Figure 3 also suggests a particular sequence to the dynamics of integrin recruitment to developing focal adhesions. As the tension builds in the stress fiber attached to the focal adhesion, the system travels along the  $\Phi$ -axis. Based on our mixed-cluster model, we suggest that this phase of tension-buildup drives a shift in FA composition, or at least in the partitioning of those integrins that are bound to the substrate. Younger focal adhesions benefit most from bound slip-type

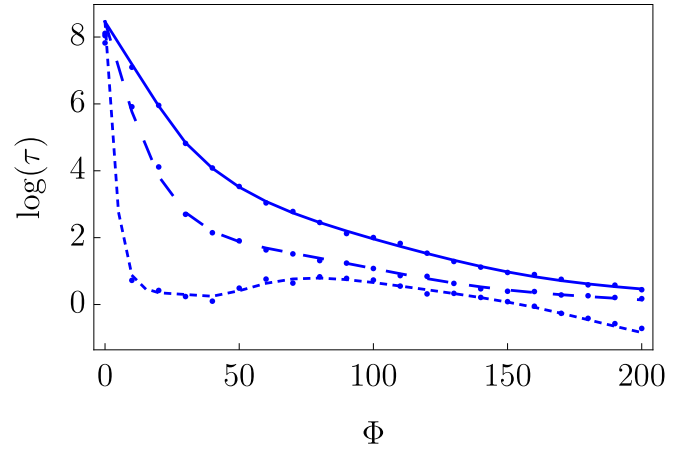


FIG. 4. Lifetimes  $\tau$  as a function of total force  $\Phi$  of mixed cluster, each consisting of 50 catch and 50 slip bonds for different relative slip bond strengths (short-dashed:  $\rho_\xi = 1$ , long-dashed:  $\rho_\xi = 3.8$ , solid line:  $\rho_\xi = 6.6$ ). In this graph, the dots represent the averaged results of 100 simulated cluster unbinding trajectories started out from  $N_c = 25$  (25 catch bonds) and  $N_s = 25$  (25 slip bonds). The three solid lines represent the corresponding analytical solutions  $T_{25,25}(\Phi)$  derived in the Appendix [Eq. (A1)], demonstrating good agreement between the different approaches.

integrins, whereas mature focal adhesions will rely more on catch bonds.

As Fig. 4 shows, the overall behavior of a mixed cluster is highly dependent upon the relative binding strength of the slip bonds in the cluster. Increasing the relative slip bond strength  $\rho_\xi$ , we see that only the mixed cluster with fast-unbinding slip bonds ( $\rho_\xi = 1$ ) shows catch bonding at the collective, cluster level. In both of the systems with relatively stronger slip bonds ( $\rho_\xi = 3.8$  and  $6.6$ ), the entire cluster behaves essentially like a slip bond even though it is largely composed of individual catch bonds. This observation may go some way toward understanding why the seemingly conflicting findings for particularly the  $\alpha_V\beta_3$  integrin in single-bond and collective measurements may not necessarily be mutually exclusive in the case of a heterogeneous population.

The partitioning of bound receptors will be exceedingly difficult to measure directly. Their complement—the unbound receptors—may well be a better target to validate the predicted behavior. In the following sections, we detail how careful observation of the diffusive behavior of both bond types inside the FA may reveal the force-dependent compositional shift our model predicts.

## VI. LATERAL DIFFUSION OF CATCH AND SLIP BONDS IN THE ADHESIVE ZONE

Why should the force-dependent composition of a mixed-cluster adhesion affect the mean diffusivity of integrins inside a FA? To see this, consider an area densely covered with integrins of both types, some bound and some unbound. The hopping of one integrin in the membrane plane to some neighboring site then requires it to exchange places with a neighbor that is also not bound, and therefore is also free to move. An abundance of bound receptors, which are immobilized by

their connection to the ECM, in this environment reduces the opportunities for such hops, and thus strongly suppresses the diffusivity of unbound integrins. Indeed, single-protein tracking experiments [29] report clear changes in the diffusivity depending on the applied tension. To model the diffusion, we include now the spatial distribution of integrins in our model by putting the integrins on a square lattice, with lattice spacing  $\lambda$ . Note, that we neglect several factors that are also likely to affect the diffusion of integrins in FAs. In particular, local crowding and specific, nonsteric interactions between the integrins will affect both the rate and the nature of the motion. However, since lateral membrane diffusion will always require free space for the diffusing species to move to, we expect that both species will be similarly affected by those factors that we do not consider. Also, the reference values for the diffusion constants, which we use from [29], are measured inside focal adhesions and should therefore be considered effective values already accounting for crowding and interactions.

In these simulations, the binding and unbinding behavior is modeled as it was before in the Gillespie approach, but now we include the spatial dimension by adding, as a potential update move, the exchange of integrin positions between two neighboring lattice sites provided both are occupied and unbound. In such a simulation, the effective in-plane diffusion coefficient  $D$  may be computed following [30] as the coefficient of proportionality between the mean residence time at a lattice site  $\langle t_{\text{res}} \rangle$  and the squared lattice spacing,

$$D = \frac{\lambda^2}{2d \langle t_{\text{res}} \rangle}, \quad (15)$$

where  $d = 2$  is the dimensionality of the lattice. For a single, unbound integrin on an otherwise empty lattice, the transition rate  $r_0$  for hopping between neighboring sites is then given by

$$r_0 = \frac{D_0}{\lambda^2}. \quad (16)$$

We shall refer to  $D_0$  as the free diffusion constant. A typical simulation for many binding and unbinding integrins of both types then proceeds as follows: neighboring unbound receptors exchange sites at a rate  $r_0$ . To be able to associate actual numbers with the quantities we compute, we choose the lattice spacing  $\lambda$  such that the total density  $\rho_{\text{tot}}$  of integrins matches the value reported in [11] ( $\rho_{\text{tot}} \approx 2500/\mu\text{m}^2$ ), which fixes  $\lambda = \sqrt{1/\rho_{\text{tot}}} \approx 20$  nm. The diffusion coefficient for free, unbound receptors is set to  $D_0 = 0.32 \mu\text{m}^2/\text{s}$  [29]; together these two numbers fix the hopping rate  $r_0$  and allow us to interpret the results of the simulations in terms of actual numbers. In our simulations, we implement excluded volume interactions: exchanges are only permitted if the receptors occupying both neighboring sites are not bound. We then measure how long each receptor spends at a single lattice site before moving to the other site to compute the residence times  $t_{\text{res}}$ . Averaging these times over all bonds of a single type (catch or slip), we compute the mean residence time for both,  $\langle t_{\text{res},c/s} \rangle$ , from which according to Eq. (15) for a 2D system the diffusion coefficients may be computed as

$$D_{c/s} = \frac{\lambda^2}{4 \langle t_{\text{res},c/s} \rangle}. \quad (17)$$

The diffusion coefficient for either bond type, in a system with a given number of catch and slip bonds, is determined by two factors: how many bonds of a given type are able to move (i.e., are unbound), and how many unbound neighbors of either type are in the direct vicinity. Figure 5 shows the resulting behavior. Dots in the three panels represent simulation data and show that for all values of the relative slip bond strength  $\rho_\xi$ , the changing composition of the cluster, as the force rises, is indeed reflected directly in the diffusive behavior of the free integrins. Initially, in all cases, the mobility of the catch bonds is considerably higher, reflecting the fact that many of them are not yet bound and thus able to diffuse. The slip bonds, in contrast, are mostly bound, and thus a large fraction of them are immobile. As the force increases this picture is reversed, and while the slip bonds are, on average, becoming increasingly mobile, more and more catch bonds are becoming bound and immobile. Interestingly, the case with the weakest slip bonds ( $\rho_\xi = 1$ ) shows a small regime of qualitatively different behavior, which may be understood from the fact that for this system—as Fig. 2(a) shows—there is initially a phase of rapid unbinding of slip bonds, which free up a lot of space for the bound catch receptors to explore. Initially, at low forces, this freeing up of additional space outpaces the additional binding of the catch receptors and, on average, increases their diffusion coefficient. This, too, illustrates how the diffusion of the unbound receptors, by virtue of their complementarity to their bound counterparts, may inform on the individual bound fractions of both types of integrins.

This simple physical picture can be summarized in the following formula for the effective, force-dependent diffusion coefficient of catch and slip integrins in adhesion sites densely covered in integrins:

$$D_{c/s}(\Phi) = D_0(1 - n_{c/s}(\Phi)) \left[ 1 - \frac{N_{\text{ct}} n_c(\Phi)}{N_{\text{ct}} + N_{\text{st}}} - \frac{N_{\text{st}} n_s(\Phi)}{N_{\text{ct}} + N_{\text{st}}} \right], \quad (18)$$

where  $n_c(\Phi)$  and  $n_s(\Phi)$  are the fraction of bound catch or slip bonds, respectively. The term between the large parentheses accounts for the availability of nonbound receptors to attempt a move, while the term between the square brackets accounts for the availability of nonbound neighbors with which to exchange positions. The predictions of Eq. (18), after plugging in the equilibrium values of  $n_c(\Phi)$  and  $n_s(\Phi)$  computed earlier, are graphed with solid lines in Fig. 5, confirming the agreement with our simulations. Comparing Fig. 5 with Fig. 2 confirms the intuitive correspondence between diffusivity and the bound/unbound fractions of both species.

## VII. DISCUSSION

We have studied the behavior of adhesive clusters composed of a mixture of catch and slip bonds. Our results show that such mixed clusters provide differential functionality compared to either of the two pure systems—the bonds, in fact, complement each other in the sense that the addition of slip bonds provides additional stability at low forces to purely catch systems (which may be helpful in some, but certainly not all, biological settings), and that the addition of catch bonds provides increased load-bearing capacity and strength at higher forces. While our model does not include direct

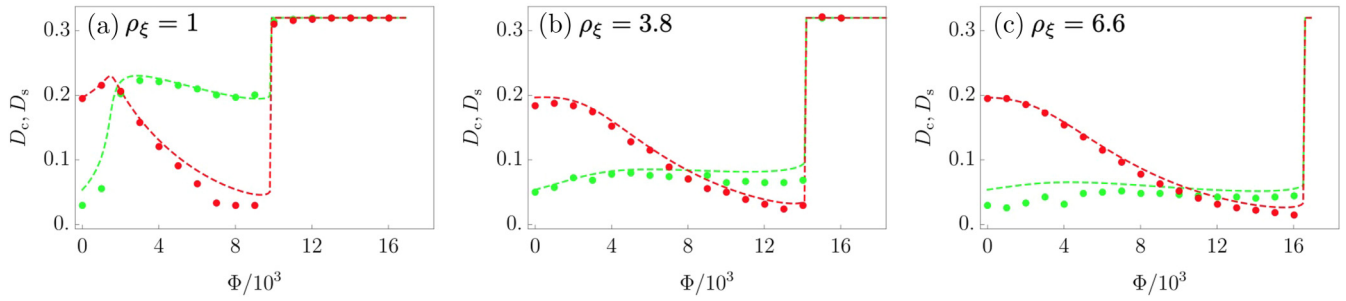


FIG. 5. Averaged diffusion constants of catch ( $D_c$ , red) and slip ( $D_s$ , green) bonds in units of  $\mu\text{m}^2/\text{s}$ , computed using Eq. (17), as a function of the total force  $\Phi$  exerted on the cluster, and for different values of the relative slip bond strength. (a)  $\rho_\xi = 1$ , (b)  $\rho_\xi = 3.8$ , and (c)  $\rho_\xi = 6.6$ . Dots are simulation results, and solid lines are calculated from approximate Eq. (18). All of the simulations were done for a system of 2048 catch bonds and 2048 slip bonds, with a rebinding rate  $\gamma = 1$ , and at  $u_{\text{sb}} = 1$ . Past the critical force for cluster unbinding, all receptors are unbound and assume their free diffusion constant  $D_0 = 0.32 \mu\text{m}^2/\text{s}$ .

interactions between the two types of bonds, they *do* interact indirectly, via the shared force.

As a result of this indirect, nonlinear coupling between the bond types, the fractions of bound receptors, for both species, change as the force is increased. Our model, therefore, suggests that the two types of bonds not only play different roles within a composite cluster, but that they are also differentially engaged depending on the applied force. Because the force exerted at a given focal adhesion increases as the adhesion matures, this implies that the engagement (or activation) of different integrin species automatically becomes organized in time, with early adhesions featuring mostly bound slip bonds and late-stage adhesion featuring more adherent catch bonds.

In experiments, this differential engagement will be exceedingly difficult to quantify or even image directly, because all of this may happen even against a background of constant overall focal adhesion composition. What changes over time are the fractions of bonds of either type that are actually *bound* to the ECM. To circumvent this difficulty, we suggest to measure instead the average diffusion coefficient of the different types of integrins inside a focal adhesion, which we find report directly on their instantaneous activation (engagement). Moreover, *changes* in these diffusion coefficients might be used to assess force-dependent changes in the contributions of these different species. While to be sure this is still by no means straightforward, it has actually been demonstrated in previous experiments [29]. Our results show that similar measurements executed at different times can compare nascent, early, and mature focal adhesions, and they have the potential to verify the differential engagement of various integrin types during adhesion cluster maturation. Again, we stress that engagement and concentration are two distinct quantities; the presence of an integrin does not imply its state of activation.

While it is most certainly oversimplifying the spectacular biophysics of the focal adhesion, our model is an attempt to quantitatively assess potential benefits of complexity and redundancy in cellular adhesion. We have focused on the case of integrins, but equally strong (and perhaps stronger) cases for the simultaneous presence of catch and slip bonds may be made for P-selectin mediated adhesion in cell rolling [26] as well as cadherin-mediated adhesions in the adherens junction [31]. We find for these general cases that even with

only two adhesive species, richer and more tunable adhesive functionalities are readily identified, that these may be intuitively understood and modeled, and that the evolution of the system is robustly self-organized—encoded through physical, statistical-mechanical principles rather than specific biochemical regulation. Experiments well within reach of the current state-of-the-art should be able to confirm some of the predictions we make here.

#### ACKNOWLEDGMENTS

This work was supported by funds from the Netherlands Organization for Scientific Research (NWO-FOM) within the program on Mechanosensing and Mechanotransduction by

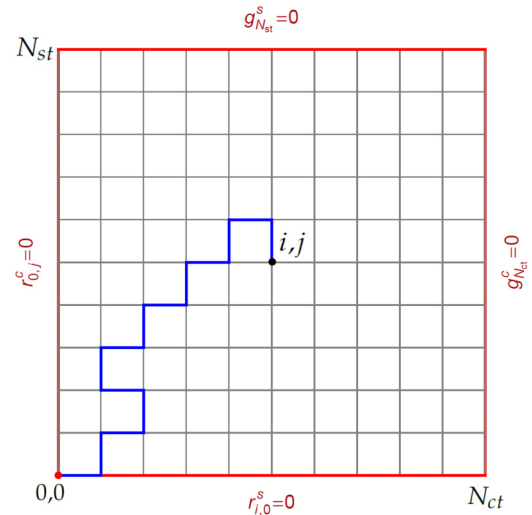


FIG. 6. Sketch of the configurational space that a cluster with two types of bonds explores. The parameters of the system are the number of bound catch bonds (along the  $x$ -axis) and the number of bound slip bonds (along the  $y$ -axis). All unbinding pathways correspond to trajectories that end up in the origin at the lower left corner. The example trajectory of unbinding (blue line) starts from  $(i, j)$  closed receptors (black point) and ends at an absorbing boundary at  $(0,0)$  (the red point); it is subject to reflecting boundaries along the red lines. The trajectory is confined to be inside the phase space at all times when  $0 \leq i \leq N_{\text{st}}$  and  $0 \leq j \leq N_{\text{ct}}$ .

Cells (FOM-E1009M). We thank Ulrich Schwarz, Erik Danen, Thorsten Erdmann, and Emrah Balcioglu for valuable discussions.

#### APPENDIX A: ANALYTICAL CALCULATION OF THE LIFETIME OF A MIXED CLUSTER

The time  $T_{i,j}$  that it takes a cluster of  $i$  bound catch and  $j$  bound slip bonds to reach the point where all catch and slip bonds are unbound obeys a recursive equation that may be derived using the methods set out in [32]. This relation reads

$$T_{i,j} = T_{i+1,j} \frac{g_i}{g_i + g_j + r_{i,j}^c + r_{i,j}^s} + T_{i,j+1} \frac{g_j}{g_i + g_j + r_{i,j}^c + r_{i,j}^s} + T_{i,j-1} \frac{r_{i,j}^s}{g_i + g_j + r_{i,j}^c + r_{i,j}^s} + T_{i-1,j} \frac{r_{i,j}^c}{g_i + g_j + r_{i,j}^c + r_{i,j}^s} + \frac{1}{g_i + g_j + r_{i,j}^c + r_{i,j}^s}, \quad (\text{A1})$$

with  $g$  and  $r$  the binding and unbinding rates as defined in the main text. The last term in Eqs. (A1) corresponds to the time that it takes to leave state  $i, j$  to any of its neighboring states in configurational space, and the first four terms represent the lifetimes of those four neighboring states, multiplied by the transition probabilities to those states (see Fig. 6). Writing this out for all possible combinations of catch and slip bonds, one obtains  $(N_c + 1) \times (N_s + 1)$  equations for  $T_{i,j}$ . This system

of coupled algebraic equations is to be solved subject to a number of boundary conditions:

$$T_{0,0} = 0 : \text{ absorbing boundary,} \quad (\text{A2})$$

$$T_{-1,0} = 0 : \text{ no negative } i, \quad (\text{A3})$$

$$T_{0,-1} = 0 : \text{ no negative } j, \quad (\text{A4})$$

$$g_{N_s}^s = 0 : \text{ reflecting boundary,} \quad (\text{A5})$$

$$g_{N_c}^c = 0 : \text{ reflecting boundary,} \quad (\text{A6})$$

$$r_{i,0}^s = 0 : \text{ reflecting boundary,} \quad (\text{A7})$$

$$r_{0,j}^c = 0 : \text{ reflecting boundary.} \quad (\text{A8})$$

Equation (A2) reflects that the cluster does not rebind after all its bonds are unbound. Equations (A3) and (A4) express the condition that the number of closed receptors is never negative. Equations (A5) and (A6) ensure that the cluster cannot rebind more bonds than are available, and finally Eqs. (A7) and (A8) ensure that the rupture rates vanish when no bonds of each type are bound.

The analytical expression for the solution of system (A1) is quite bulky, and it cannot be expressed in a compact form for each of the  $T_{i,j}$ . However, Eq. (A1) is straightforwardly solved for a given total number of catch and slip bonds. These solutions are graphed in Fig. 4, where we calculate the lifetime of a cluster consisting of 50 catch bonds and 50 slip bonds with various parameters, and we confirm the analytical outcome by comparing to stochastic simulations.

- 
- [1] C.-M. Lo, H.-B. Wang, M. Dembo, and Y.-I. Wang, *Biophys. J.* **79**, 144 (2000).
- [2] D. Discher, P. Janmey, and Y.-L. Wang, *Science* **310**, 1139 (2005).
- [3] H. J. Kong, J. Liu, K. Riddle, T. Matsumoto, K. Leach, and D. J. Mooney, *Nat. Mater.* **4**, 460 (2005).
- [4] J. Z. Keckhagia, J. Ivaska, and P. Roca-Cusachs, *Nat. Rev. Mol. Cell Biol.* **20**, 457 (2019).
- [5] P. Kanchanawong, G. Shtengel, A. M. Pasapera, E. B. Ramko, M. W. Davidson, H. F. Hess, and C. M. Waterman, *Nature (London)* **468**, 580 (2010).
- [6] C. Cluzel, F. Saltel, J. Lussi, F. Paulhe, B. A. Imhof, and B. Wehrle-Haller, *J. Cell Biol.* **171**, 383 (2005).
- [7] P. Roca-Cusachs, N. C. Gauthier, A. del Rio, and M. P. Sheetz, *Proc. Natl. Acad. Sci. (USA)* **106**, 16245 (2009).
- [8] C. Diaz, S. Neubauer, F. Rechenmacher, H. Kessler, and D. Missirlis, *J. Cell Sci.* **133**, jcs232702 (2020).
- [9] D. P. White, P. T. Caswell, and J. C. Norman, *J. Cell Biol.* **177**, 515 (2007).
- [10] H. E. Balcioglu, H. van Hoorn, D. M. Donato, T. Schmidt, and E. H. J. Danen, *J. Cell Sci.* **128**, 1316 (2015).
- [11] A. Elosegui-Artola, E. Bazellieres, M. D. Allen, I. Andreu, R. Oria, R. Sunyer, J. J. Gomm, J. F. Marshall, J. L. Jones, X. Trepat *et al.*, *Nat. Mater.* **13**, 631 (2014).
- [12] F. Kong, A. J. Garcia, A. P. Mould, M. J. Humphries, and C. Zhu, *J. Cell Biol.* **185**, 1275 (2009).
- [13] D. Boettiger, L. Lynch, S. Blystone, and F. Huber, *J. Biol. Chem.* **276**, 31684 (2001).
- [14] G. Jiang, G. Giannone, D. R. Critchley, E. Fukumoto, and M. P. Sheetz, *Nature (London)* **424**, 334 (2003).
- [15] Y. Chen, H. Lee, H. Tong, M. Schwartz, and C. Zhu, *Matrix Biol.* **60**, 70 (2017).
- [16] R. I. Litvinov, V. Barsegov, A. J. Schissler, A. R. Fisher, J. S. Bennett, J. W. Weisel, and H. Shuman, *Biophys. J.* **100**, 165 (2011).
- [17] S. Walcott and S. X. Sun, *Proc. Natl. Acad. Sci. (USA)* **107**, 7757 (2010).
- [18] Ph. Marcq, N. Yoshinaga, and J. Prost, *Biophys. J.* **101**, L33 (2011).
- [19] U. S. Schwarz, T. Erdmann, and I. Bischofs, *Biosystems* **83**, 225 (2006).
- [20] T. Erdmann and U. S. Schwarz, *Phys. Rev. Lett.* **92**, 108102 (2004).
- [21] U. S. Schwarz and T. Erdmann, *Eur. Phys. J. E* **22**, 123 (2007).
- [22] E. A. Novikova and C. Storm, *Biophys. J.* **105**, 1336 (2013).
- [23] H. A. Kramers, *Physica VII* **4**, 284 (1940).
- [24] M. Dembo, D. Torney, K. Saxman, and D. Hammer, *Proc. R. Soc. B* **234**, 55 (1988).
- [25] Y. V. Pereverzev, O. V. Prezhdo, M. Forero, E. V. Sokurenko, and W. E. Thomas, *Biophys. J.* **89**, 1446 (2005).
- [26] B. T. Marshall, M. Long, J. W. Piper, T. Yago, R. P. McEver, and C. Zhu, *Nature (London)* **423**, 190 (2003).

- [27] D. Nordin, L. Donlon, and D. Frankel, *Soft Matter* **8**, 6151 (2012).
- [28] D. T. Gillespie, *J. Phys. Chem.* **81**, 2340 (1977).
- [29] O. Rossier, V. Oceau, J.-B. Sibarita, C. Leduc, B. Tessier, D. Nair, V. Gatterdam, O. Destaing, C. A. s Rizo, R. Tampé *et al.*, *Nat. Cell Biol.* **14**, 1057 (2012).
- [30] J. W. Haus and K. W. Kehr, *Phys. Rep.* **150**, 263 (1987).
- [31] S. Rakshit, Y. Zhang, K. Manibog, O. Shafraz, and S. Sivasankar, *Proc. Natl. Acad. Sci. (USA)* **109**, 18815 (2012).
- [32] N. V. Kampen, *Stochastic Processes in Physics and Chemistry* (North-Holland, Amsterdam, 1987).